THE INFLUENCE OF LAMINATION AND CONDUCTIVE PRINTING INKS ON SMART-CARD OPERABILITY

VPLIV LAMINACIJE IN PREVODNIH TISKARSKIH BARV NA DELOVANJE PAMETNIH KARTIC

Miloje Đokić[1], Vasa Radonić[2], Vladan Mladenović[3], Anton Pleteršek[4], Urška Kavčič[5], Aleš Hladnik[1], Vesna Crnojević-Bengin[2], Tadeja Muck[1]

[1]Faculty of Natural Sciences and Engineering, University of Ljubljana, Snežniška 5, 1000 Ljubljana, Slovenia
[2]Faculty of Technical Sciences, University of Novi Sad, Trg Dositeja Obradovića 6, 21000 Novi Sad, Serbia
[3]Cetis, d. d., Čopova ulica 24, 3000 Celje, Slovenia
[4]ams R&D, d. o. o., Tehnološki park 21, 1000 Ljubljana, Slovenia
[5]Valkarton Rakek, d. o. o., Partizanska cesta 7, 1381 Rakek, Slovenia
miloje.djokic@gmail.com

In this paper a novel design of UHF RFID antennas for smart cards is proposed. Smart cards usually include HF RFID antennas produced by means of hot foil stamping or etching – a subtractive process. Making HF antennas using printing – an additive process – is difficult, because it necessitates the printing of three layers: that of conductive lines (a coil), followed by a dielectric layer and once again a conductive layer. On the other hand, the printing of UHF antenna requires only the single-layer printing of conductive lines, i.e., antenna, thus enabling a more rational printing.

After designing, simulating and testing a folded UHF dipole antenna for RFID applications, the impact of three different conductive printing inks, reading distance and card deformation on the backscattered signal power was studied. A three-way analysis of variance (ANOVA) was implemented to aid in the interpretation of the measurement results obtained on both non-laminated and laminated cards. It was demonstrated that smart cards with screen-printed UHF antennas can be fabricated using the proposed design optimization, so achieving good card readability.

Keywords: smart cards, printed antenna, antenna design, lamination, conductive printing inks, UHF RFID, analysis of variance

V članku je predlagana nova izvedba UHF RFID-anten za pametne kartice. Pametne kartice navadno vključujejo HF RFID-antene, izdelane na podlagi vročega tiska s folijo ali z jedkanjem (subtraktivni proces). Izdelava HF-anten v tisku (aditivni proces) je težavna, saj mora biti tisk izveden v treh plasteh – tisk prevodnih linij (tuljava), dielektrične plasti in nato ponovno prevodne plasti. Po drugi strani pa je želen enoplastni tisk prevodnih linij UHF-antene, kar omogoča racionalnejši tisk.

Po načrtovanju, simulaciji in preizkušanju dipolne UHF-antene za RFID-aplikacije je bil preučevan vpliv treh prevodnih tiskarskih barv, razdalje odčitavanja in deformacije kartic na moč povratnega signala. Pri razlagi dobljenih rezultatov meritev nelaminiranih in laminiranih kartic je bila uporabljena trosmerna analiza variance (ANOVA). Izkazalo se je, da je mogoče izdelati pametne kartice s tehniko sitotiska z opisano optimizacijo izvedbe UHF-antene, kar omogoča dobro čitljivost kartic.

Ključne besede: pametne kartice, tiskana antena, izvedba antene, laminacija, prevodne tiskarske barve, UHF RFID, analiza variance

1 INTRODUCTION

Printed flexible electronics is becoming more viable with recent technological developments, opening up possibilities to integrate radio frequency (RF) functions into clothing or moving objects to monitor various parameters of interest. Printed electronics that combine electronic components with different printing technologies allows the production of miniature low-cost electronic systems.

The first connection between printing technology and conventional electronics appeared in the 1980s when Teng and Vest made metal conductors for solar cells using inkjet printing.[1] This opened up the possibility to produce various electronic components using different printing techniques. Generally, two printing techniques are the most common, i.e., screen printing[2–8] and inkjet printing,[9–12] but others such as flexography,[13] gravure printing[14] and pad printing[15] are also used. Conventional printing techniques, such as screen printing or gravure printing, are characterized by high production speed, high resolution and the possibility of using a number of different conductive inks, so these techniques are suitable for the mass production of precise electronics.[11] Printed electronics has many advantages, including a simple production process, the reduced consumption of raw materials and high productivity (especially in roll-to-roll processes). One of the major applications of printed electronics is radio-frequency identification (RFID). RFID is an automatic identification technology that uses a wireless non-contact radio frequency to transfer data for the purposes of automatically identifying and tracking the tags attached to objects. RFID systems are widely used in various real-life applications, such as access control or smart-card systems, public transport and logistics.[16–18] RFID systems consist of at least of a reader, which receives the feedback signals sent back from the tags, and the tags themselves. The simplest, passive tags consist of an antenna and an integrated

circuit (IC). An integrated controller and a memory in the IC chip enable the activity of the tag and contain electronically stored information. The second part of the tag is the antenna that receives and transmits the radio signals.

Since the mechanical and electrical characteristics of antennas depend on the materials used, several experimental studies have recently been carried out to investigate the effects of conductive pastes,[3] to compare different printed materials[19] and to look at the influence of substrate folding.[12] The effects of different materials used in the production of UHF RFID antennas on their performance have been analysed.[19] It has been shown that the conductive material used to print the antenna has a significant influence on the antenna's return loss. A similar study has confirmed that a conductive silver-based paste outperformed all the other types of conductive pastes and provided a performance similar to that of its copper equivalent.[3]

This paper presents a novel design for UHF RFID smart cards, realized using the basic functionality offered by printing technology. The impacts of different conductive inks that are used to print the UHF antenna are investigated. In addition, the influence of the lamination process and card deformation on the performance of the cards is investigated in detail.

2 THEORETICAL

The reading range in the free space of an RFID system operating at wavelength λ depends on the reader power density (P_{TX}^{rdr}), the antenna gain (G_{rdr}) and the tag antenna gain (G_{tag}). The power received by the tag (P_{RX}^{tag}) at distance r from the reader is estimated using the Friis equation:[20]

$$P_{RX}^{tag} = P_{TX}^{rdr} G_{rdr} G_{tag} \left(\frac{\lambda}{4\pi r}\right)^2 \tag{1}$$

The transmitted signal power is denoted by TX, while the received signal is denoted by RX. We can define the gain of the tag antenna G_{tag} and the backscatter transmission loss T_b using the relationships from the Friis equation, as expressed in equations Eq. 2 to 4:

$$P_{TX}^{tag} = P_{TX}^{rdr} G_{rdr} G_{tag} \left(\frac{\lambda}{4\pi r}\right)^2 T_b \tag{2}$$

$$P_{RX}^{rdr} = P_{TX}^{tag} G_{tag} G_{rdr} \left(\frac{\lambda}{4\pi r}\right)^2 \tag{3}$$

$$P_{RX}^{rdr} = P_{TX}^{rdr} T_b G_{rdr}^2 G_{tag}^2 \left(\frac{\lambda}{4\pi r}\right)^4 \tag{4}$$

The backscattered modulated signal received by the reader is therefore proportional to r^{-4}. Nevertheless, the communication between the passive tag and the reader is forward link limited, since the power to power on the IC (P_{min}^{tag}) is by at least 6 orders of magnitude higher than the

minimum power (P_{min}^{rdr}) required to demodulate the backscattered signal. The forward limited range in free space ($R_{forward}$) follows from Eq. 5:

$$R_{forward}) = \left(\frac{\lambda}{4\pi}\right) \sqrt{\frac{P_{TX}^{rdr} G_{rdr} G_{tag}}{P_{min}^{tag}}} \tag{5}$$

A simple estimation for a reader with the power P_{TX} = 500 mW, a tag in the form of a $\lambda/2$ dipole, with gain G_{tag} = 2.2 dBi and minimum power needed to turn on the IC P_{min}^{tag} = 100 μW, gives a forward range of 2.4 m in free space. Until this point, a perfect matching between the antenna and load (IC) has been assumed with the power-transfer coefficient $\tau = 1$. Generally speaking, the power-transfer coefficient is defined by Eq. 6:

$$\tau = \frac{4R_{chip} R_{ant}}{\left| Z_{chip} + Z_{ant} \right|^2} \tag{6}$$

where the impedance of the chip (Z_{chip}) and the antenna (Z_{ant}) is the sum of the resistance and the reactance. The transfer coefficient is a maximum when the reactance of the chip and antenna cancel each other. In this case, referred to as conjugate matching, the transfer coefficient is equal to 1. In all other cases, the transfer coefficient is lower.

The effective gain (G_{eff}) of the tag antenna (the ability to increase the power or amplitude of the signal) can be defined as follows[6]:

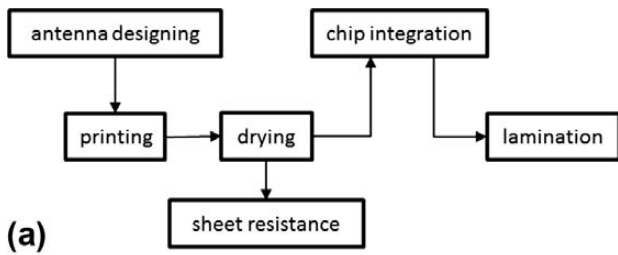$$\tau G_{eff} = D\eta\tau \tag{7}$$

where D is the directivity of the antenna, η is the antenna efficiency and τ is the power transfer efficiency.
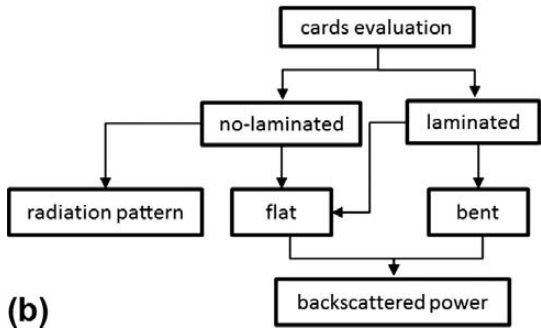
3 EXPERIMENTS

The block diagram of the smart-card fabrication process is shown in **Figure 1a**. First, the UHF antenna was designed using the EM simulator CST Microwave Studio and then printed and dried. In the next step, the chips were assembled and the lamination performed to fabricate a final smart card. The fabricated cards were experimentally tested following the process shown in **Figure 1b**. The characteristics of the flat non-laminated antenna were measured in an anechoic chamber, while the backscattering characteristics of the smart cards were evaluated in a real environment using an ams-R902 reader. Furthermore, the effect that bending has on the initial planar topology in the case of the laminated cards was also investigated. Multifactorial analysis of variance (ANOVA) was implemented to aid in the interpretation of the measurement results obtained for both non-laminated and laminated cards.

3.1 Antenna design and simulation

The novel design configuration of the proposed folded dipole antenna is shown in **Figure 2**. The antenna

Figure 1: a) Block diagrams of smart-card fabrication, b) testing and measurement process
Slika 1: a) Blokovna diagrama izdelave pametnih kartic, b) procesa preizkušanja in merjenja

Figure 3: Cross section of the laminated card with antenna placed inside
Slika 3: Prečni prerez laminirane kartice z vključeno anteno v vmesni plasti

Figure 4: Simulated return losses of the laminated and non-laminated antennas
Slika 4: Simulacija izgube povratnega signala laminirane in nelaminirane antene

is designed to operate according to the UHF standard with a central operating frequency of 868 MHz. In addition, the dipole is folded in order to fit the standard credit-card size, with a negligible reduction in antenna efficiency. The antenna was designed for a thick polycarbonate film 120 µm (grammage: 120 g/m^2; surface roughness, ISO 4288: 2.3 µm) with a relative permittivity of ε_r = 3.2 and a dissipation factor 0.0019. All the simulations were performed using CST Microwave Studio. For the conductive material, 16 µm silver was used and the conductor losses were modelled using the bulk conductivity for silver.

As the number and thickness of the dielectric layers during lamination affects the characteristics of the antennas, initially the antenna dimensions were determined for
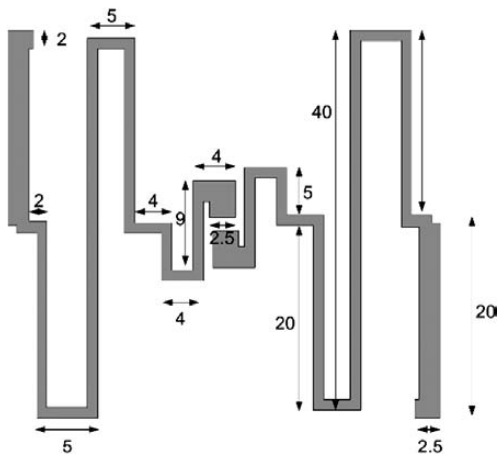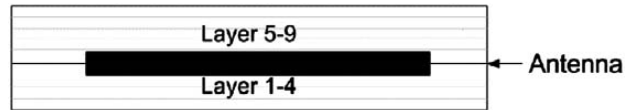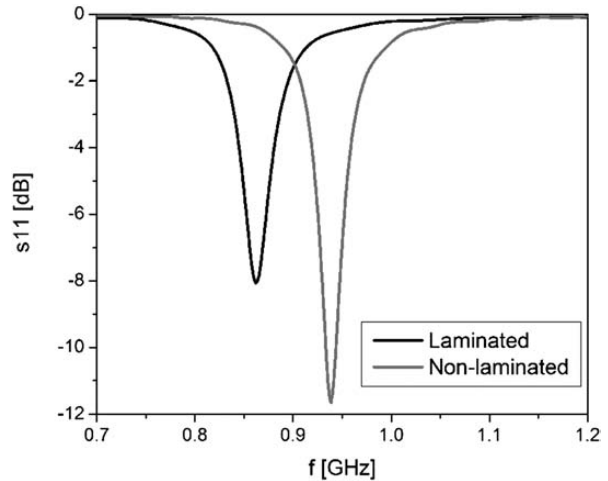
the laminated case. Nine dielectric layers were used in the simulation, with the antenna placed between the fourth and fifth layers (**Figure 3**).

The dimensions of the antenna are carefully optimized in order to obtain the central frequency of 868 MHz. The final antenna dimensions are shown in **Figure 2**, with all the marked dimensions in mm. The total antenna size is only 37 mm × 41 mm. **Figure 4** compares the simulated return loss of the laminated and non-laminated antennas. It is clear that the lamination process significantly influences the resonant frequency of the antenna,
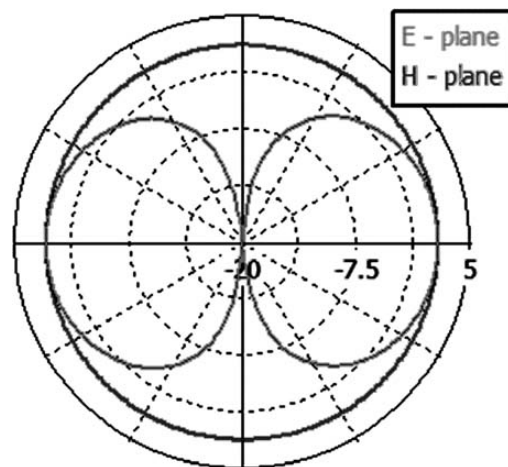

Figure 2: Proposed folded dipole antenna (mm)
Slika 2: Nova izvedba dipolne antene (mm)

Figure 5: Simulated radiation pattern of the laminated antenna
Slika 5: Simulacija sevalnega diagrama laminirane antene

due to changes in the effective dielectric constant of the substrate.

The simulated radiation patterns of the proposed laminated dipole antenna in the *E*- and *H*-planes are shown in **Figure 5**. The total antenna gain is above 1.9 dBi.

3.2 Printing and drying

Antenna samples were printed using the Siasprint Novaprint-P screen printer with a monofilament polyester plain weave mesh with 120 l/cm and a theoretical ink volume of 16.3 cm^3/m^2. For printing, three different silver conductive printing inks were used:

- SC-CRSN2442 SunTronic 280 Thermal Drying Silver Conductive Ink,
- DP-DuPont 5064H Silver Conductor,
- UV-Electra Polymers ELX 30.

Inks denoted as SC and DP require thermal drying, while UV is an ultraviolet curing ink. The characteristics of the used inks are summarized in **Table 1**.

After printing, the optimal drying process for each ink was determined. The optimal drying was determined as the point where the sheet resistance of the printed samples became constant and did not get any lower with a longer drying time, higher temperature or higher or longer UV exposure. In accordance with the SC and DP printing inks' specifications, drying in an infra-red (IR) tunnel was performed. The best results – the lowest sheet resistance – were obtained when the samples passed the IR tunnel seven times (at 72 °C for 30 s). The UV printed samples were optimally cured when twice passed through a UV tunnel with a dose of 700 mJ/cm^2.

3.3 Sheet resistance

The resistance, *R*, of the printed conductive lines was measured using a DT-890G digital multimeter on the test element, as shown in **Figure 6**, between points 1 and 2. The nominal length, *L*, between points 1 and 2 was 22 mm and the line width, *W*, was set to 3 mm. The resistance was measured after 24 h of conditioning with a 50 % relative humidity at 23 °C. The nominal number of
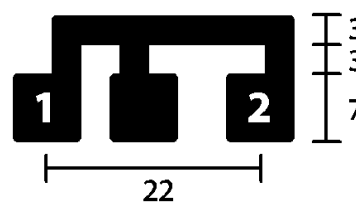

Figure 6: Test element for resistance measurements
Slika 6: Preizkusni element za merjenje upornosti

squares N_{sq} and the final sheet resistance R_{sh} of the conductive ink layer (mΩ) can be calculated using Eq. 8 and Eq. 9, respectively. The measured resistances for the different inks are shown in **Table 1**.

$$N_{SQ} = \frac{L}{W} = 10.3 \qquad (8)$$

$$R_{sh} = \frac{R}{N_{SQ}} \qquad (9)$$

3.4 Chip integration

In our study, NXP strap chips were used. The main chip characteristics are as follows: operating frequency 840–960 MHz, impedance 22 – j195 Ω and *Q*-factor 9. The chips were assembled with isotropic conductive glue based on silver particles (Bison, Netherlands) after the drying process. After chip integration, tags were dried in a thermal oven at 120 °C for 30 min.

3.5 Lamination

The lamination process was used to fabricate the final smart cards. It was separated into two phases: first the "heat phase", where nine foil layers were assembled at a temperature of 199 °C and a pressure of 300 N/cm^2 for a fixed period of 19 min. In the second phase, the "cold phase", the assembled foils were exposed to 25 °C and a pressure of 500 N/cm^2 for 18 min. Finally, cutting into final cards sized according to ISO/IEC 7810 standard was carried out. The final prototype of the laminated smart card is shown in **Figure 7**.

Table 1: Properties of investigated printing inks
Tabela 1: Lastnosti tiskarskih barv

Printing ink	Solids (%)	Recommended drying condition	Specified resistance* R_{sh} (spec.)/mΩ (layer thickness)	Measured resistance** R_{sh} (meas.)/mΩ
SC CRSN2442 SunTronic 280	69–71	100–130 °C over 30–90 s in the hot zone	10–32 (25 μm)	118.12
DP DuPont 5064H	63–66	140 °C over 120 s in the hot zone	≤ 6 (25 μm)	567.96
UV Electra Polymers ELX 30	approx. 75	1000–1500 mJ cm^{-2}	300–500 (15 μm)	653.72

*Sheet resistance from the product specification
**Sheet resistance measured on printed samples using the DT-890G digital multimeter. An average thickness of 15 μm was determined on the prints' cross-sections with a scanning electron microscope.
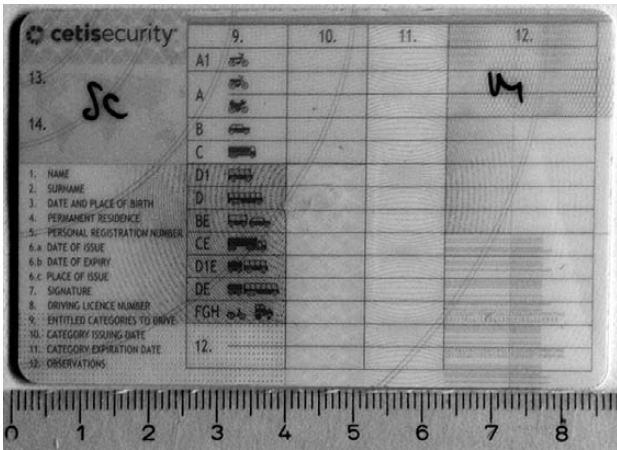
Figure 7: Final laminated smart card prototype
Slika 7: Končni prototip laminirane pametne kartice

4 RESULTS AND DISCUSSION

4.1 Non-laminated antenna measurements

The return loss of the fabricated non-laminated SC antenna was measured and the comparison of the simulated and measured return losses for the non-laminated antenna is given in **Figure 8**, with a photograph of the fabricated circuit shown in an inset. Despite the small size of the antenna, good agreement is observed and the fundamental resonance occurs at 940 GHz, as predicted, with a reflection better than –10 dB.

Figure 9 shows the comparison of the simulated and measured radiation patterns for the non-laminated antenna. The pattern measurements were taken in an anechoic chamber using a vector network analyser and the measured patterns agree well with the simulated ones, except for some ripple, which is ascribed to reflections in the chamber.
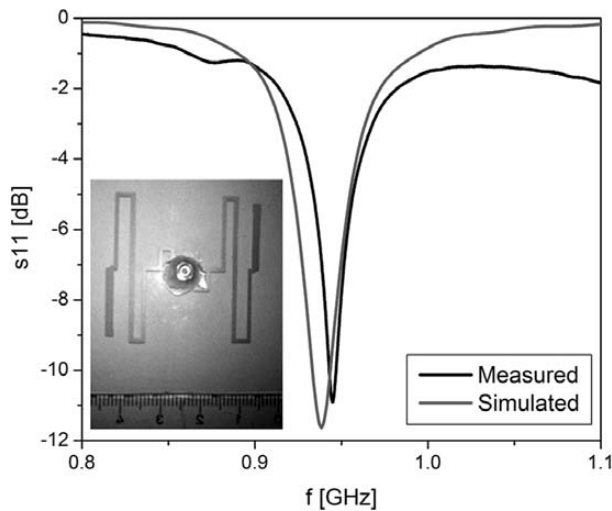

Figure 8: Comparison of simulated and measured return losses for the non-laminated antenna with inset photograph of the fabricated circuit
Slika 8: Primerjava simulirane in izmerjene povratne izgube signala za nelaminirano anteno z vključeno sliko natisnjenega vezja
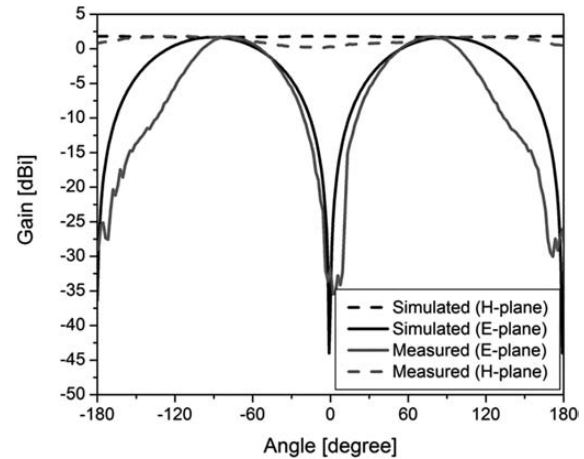

Figure 9: Comparison of simulated and measured radiation patterns in *E*-plane and *H*-plane for non-laminated antenna
Slika 9: Primerjava simuliranega in izmerjenega sevalnega diagrama v *E*-ravnini in *H*-ravnini za nelaminirane antene

4.2 Card evaluation

The realized readability of the cards with RFID tags was measured in a real environment using an IDS-R902 reader that consists of the reader electronics and an A0025 circularly polarized patch antenna (Poynting GmbH, Dortmund, Germany) with gain of 6.5 dBi emitting UHF EM radiation at frequency f = 868 MHz. The reader electronics measures the intensity of the modulated backscattered signal.

The cards with UHF RFID tags were evaluated by measuring the backscattered power (dBm), moving the tag in a straight line perpendicular to the reader in 2 cm increments, starting at 2 cm from the emitting antenna up to the estimated free space working distance (**Figure 10**).

Multifactorial (multiway) analysis of variance (ANOVA) was implemented to aid in the interpretation of the measurement results obtained for both non-laminated and laminated cards. The impact of the three selected factors on the response – backscattered power – was
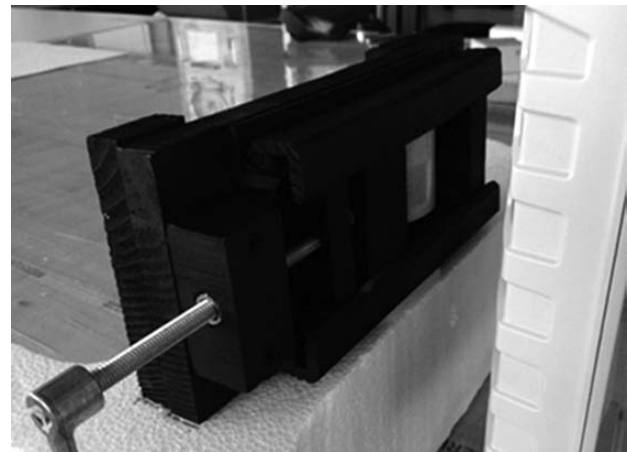

Figure 10: Measurement of the backscattered power
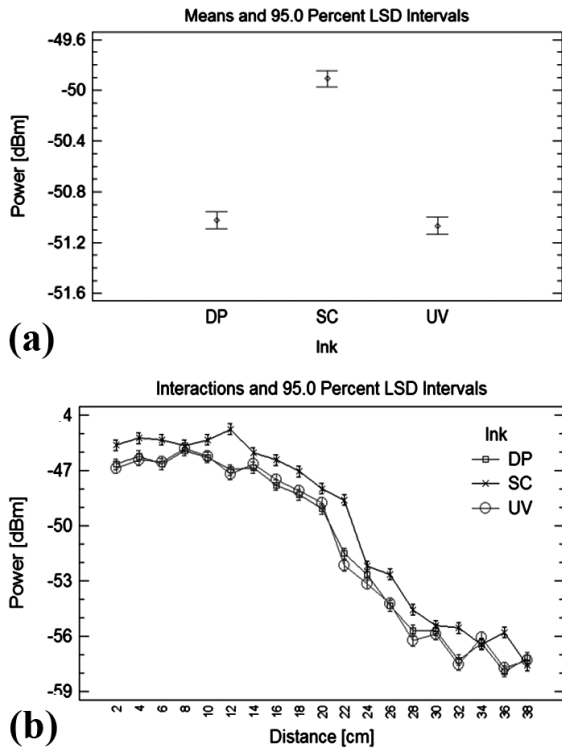**Slika 10:** Merjenje moči povratnega signala

Figure 11: Non-laminated cards: a) effect of ink type and b) ink-type/reading distance interaction on the backscattered signal power

Slika 11: Nelaminirane kartice: a) vpliv vrste tiskarske barve in b) interakcije vrsta tiskarske barve/razdalja odčitavanja na moč povratnega signala
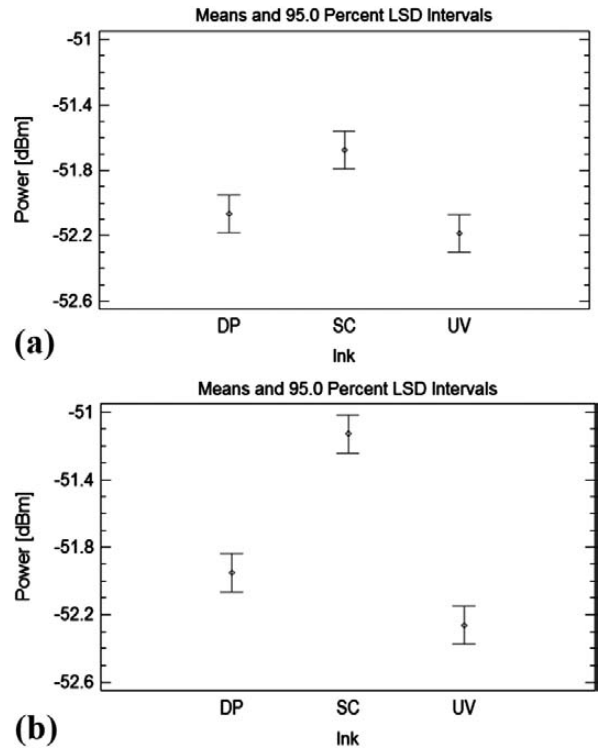

Figure 13: Laminated cards effect of ink type on backscattered power for: a) flat and b) bent cards

Slika 13: Laminirane kartice: vpliv vrste tiskarske barve na moč povratnega signala za: a) ravne in b) upognjene kartice

Figure 12: Laminated cards: a) effect of ink type and b) flatness on backscattered signal power

Slika 12: Laminirane kartice: a) vpliv vrste tiskarske barve in b) ploskosti na moč povratnega signala

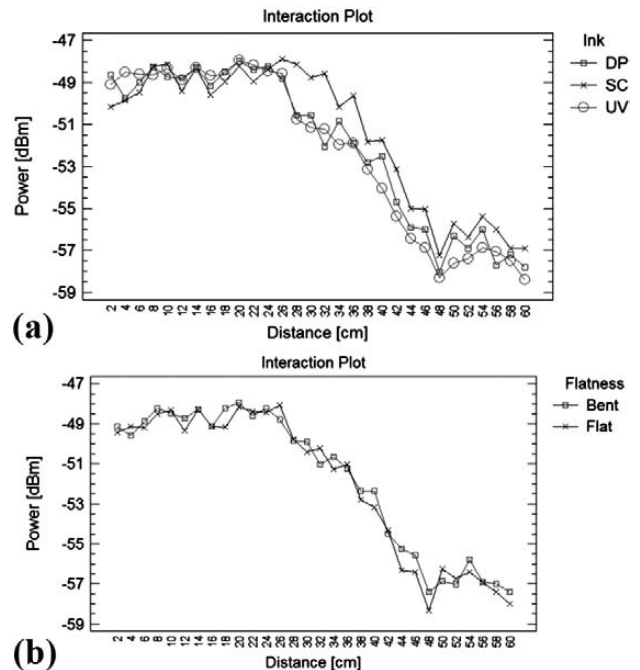**Figure 14:** Laminated cards: a) effects of interactions – ink-type/reading distance and b) flatness/reading distance on backscattered power

Slika 14: Laminirane kartice: a) vpliv interakcije vrsta tiskarske barve – razdalja odčitavanja in b) ploskost – razdalja odčitavanja na moč povratnega signala

studied: ink type, reading distance and flatness, the later one only for the laminated cards (flat or bent). The cards were bent to a final deformed position: 2.6 cm height, 3 cm width, 1.73269 cm radius and an angle of 240° subtended by an arc. The results of the statistical analysis at $\alpha = 0.05$ (i.e., a 95 % confidence level) are presented in **Figures 11a**, **12a**, **12b**, **13a** and **13b**. The analyses were made on nine samples for each of the various cards (non-laminated, flat laminated and bent laminated).

4.3 Non-laminated cards

All of the examined non-laminated cards were flat, so here only two factors – ink type and reading distance – were analysed. As shown in the ANOVA table (**Table 2a**), both factors have a statistically significant effect (*P*-value < 0.05) on the response. The very small interaction effect (*F*-ratio$_{AB}$ = 6.16) is merely due to an extremely strong impact of the reading distance and can be neglected. **Figure 11a** and the multiple range test data (**Table 2b**) clearly show that the SC ink behaves in a substantially different manner compared to the other two inks: the mean backscattered signal power of the UHF RFID cards with the applied SC ink is –49.9 dBm, while the mean responses with the DP and UV inks are –51.0 dBm and –51.1 dBm, respectively. The difference in the responses between the latter two inks is not statistically significant (**Table 2b**), since the corresponding mean values form the same homogeneous group (a). The ink type/reading distance diagram (**Figure 11b**) also supports the above findings.

4.4 Laminated cards

In addition to the impacts of the ink type and reading distance, the flatness of the substrate was studied in the case of the laminated cards. As shown in **Table 3a**,

reading distance has by far the strongest effect on the backscattered power, followed by the effects of the ink type and flatness. The impact of the three ink types on the response (**Figure 12a**) is similar to that found with the non-laminated cards, the only difference being that the mean response with the UV ink (–52.2) is now statistically higher compared to the one with the DP ink (–52.0) (**Table 3b**). The detected backscattered power with the flat cards is generally lower than with the bent cards (**Figure 12b**).

The compared maximum reading distances of the non-laminated and laminated cards showed a significant difference (presented in **Figures 11b** and **14a**). Since the antenna is designed for laminated cards, the lamination process increases the reading distance from 40 cm to 60 cm.

To find out how flatness affects the measured back-scattered power, we ran two more ANOVAs, separately for the flat and for the bend cards. The results (**Figure 13**) indicate that the differences in the effects of the DP, UV and SC inks on the response become more pronounced with bending (**Figure 13**).

It is clear that the readability of the cards depends on the conductivity of the printing ink used for printing the antenna. Antennas printed with SC ink (R_{sh} = 118.12 mΩ) had 5 to 6 times higher conductivity than those with DP and UV inks and, as a consequence, the cards printed

Table 2: Non-laminated cards: a) ANOVA table and b) multiple range test results for ink type; SS = Sum of Squares, Df = Degrees of Freedom, MS = Mean Square
Tabela 2: Nelaminirane kartice: a) ANOVA tabela in b) rezultati preizkusov večkratnih primerjav za vrsto tiskarske barve; SS = vsota kvadratov, Df = stopinje prostosti, MS = povprečje kvadratov

a)

Source	SS	Df	MS	F-Ratio	P-Value
MAIN EFFECTS					
A:Ink	302.14	2	151.07	187.25	0.0000
B:Distance	20749.4	18	1152.74	1428.83	0.0000
INTERACTIONS					
AB	178.831	36	4.96753	6.16	0.0000
RESIDUAL	781.763	969	0.806773		
TOTAL (corr.)	22063.8	1025			

b) Method: 95.0 percent Duncan

Ink	Count	LS Mean	LS Sigma	Homogen. groups
UV	323	-51.0687	0.049978	a
DP	342	-51.0228	0.048569	a
SC	361	-49.9094	0.047274	b

Table 3: Laminated cards: a) ANOVA table, b) multiple range test results for ink type and c) flatness; SS = Sum of Squares, Df = Degrees of Freedom, MS = Mean Squares
Tabela 3: Laminirane kartice: a) ANOVA tabela, b) rezultati preizkusov večkratnih primerjav za vrsto tiskarske barve in c) ravnoležnosti; SS = vsota kvadratov, Df = stopinje prostosti, MS = povprečje kvadratov

a)

Source	SS	Df	MS	F-Ratio	P-Value
MAIN EFFECTS					
A:Ink	65.2691	2	32.6346	54.48	0.0000
B:Distance	6701.27	29	231.078	385.79	0.0000
C:Flatness	5.2215	1	5.2215	8.72	0.0034
INTERACTIONS					
AB	171.159	58	2.95101	4.93	0.0000
AC	9.20544	2	4.60272	7.68	0.0005
BC	33.2657	29	1.14709	1.92	0.0036
ABC	44.609	58	0.769121	1.28	0.0912
RESIDUAL	215.633	360	0.598981		
TOTAL (corr.)	7245.63	539			

b) Method: 95.0 percent Duncan

Ink	Count	LS Mean	LS Sigma	Homogen. groups
UV	180	-52.2244	0.057686	a
DP	180	-52.0094	0.057686	b
SC	180	-51.4033	0.057686	c

c) Method: 95.0 percent Duncan

Flatness	Count	LS Mean	LS Sigma	Homogen. groups
Flat	270	-51.9774	0.0471	a
Bent	270	-51.7807	0.0471	b

with SC ink had a better readability or a higher back-scattered power (dBm) of the return signal. The maximum reading (working) distance showed no significant differences between the applied inks. Furthermore, the maximum reading distance was higher for the laminated cards, with an approximately 20 cm increase, regardless of the ink used.

With card deformation, we are assuming that the bending increases the reading distance range. This can be seen from **Figure 14b**, where the strength of the modulated backscattered signal is improved after bending. The result of the performed analysis shows that the printed cart printed with SC inks outperforms all the other printed cards in terms of the backscattered power.

5 CONCLUSIONS

In the present study, a novel folded UHF RFID antenna that requires only single-layer printing has been proposed and implemented in the smart-card design. Despite the small size of the antenna, good readability was achieved. Through optimizing the antenna design, more rational printing for low-cost mass production can be possible.

We showed that a higher ink conductivity increases the backscattered power and that the novel design of the UHF antenna is appropriate for final laminated smart cards, while the lamination process increases the maximum reading distance.

By the end of our research, we had shown that smart cards with screen-printed UHF antennas can be realized. The main effect on the final tag's operability is that of the quality of the conductive ink itself, while bending can improve the strength of the modulated backscattered signal. The study of chip contacting, especially the glue/ink interactions and the influence of the mechanical strength of smart cards, will be the topic of our future research.

Acknowledgments

6 REFERENCES

[1] K. F. Teng, R. W. Vest, Metallization of solar cells with ink jet printing and silver metallo-organic inks, IEEE Transaction on Components, Hybrids and Manufacturing Technology, 11 (**1988**), 291–297
[2] D. Y. Shin, Y. Lee, C. H. Kim, Performance characterization of screen printed radio frequency identification antennas with silver nanopaste, Thin Solid Films, 517 (**2009**), 6112–6118
[3] K. Janeczek, M. Jakubowska, G. Kozioł, A. Młozłniak, A. Araz´na, Investigation of ultra-high-frequency antennas printed with polymer pastes on flexible substrates, IET Microwaves, Antennas & Propagation, 6 (**2012**), 549–554
[4] T. Elsherbeni, K. E. Mahgoub, L. Sydanheimo, L. Ukkonen, F. Yang, Laboratory scale fabrication techniques for passive UHF RFID tags, Antennas and Propagation Society International Symposium (APSURSI), 2010 IEEE, Toronto, 2010
[5] K. Janeczek, M. Jakubowska, A. Młozłniak, G. Koziol, Thermal characterization of screen printed conductive pastes for RFID antennas, Materials Science and Engineering B: Solid-State Materials for Advanced Technology, 177 (**2012**), 1336–1342
[6] U. Kavčič, L. Pavlovič, M. Pivar, M. Đokić, B. Batagelj, T. Muck, Printed electronics on recycled paper and cardboards, Inf. MIDEM, 43 (**2013**) 1, 50–57
[7] U. Kavčič, M. Maček, T. Muck, M. Klanjšek Gunde, Readability and modulated signal strength of two different ultra-high frequency radio frequency identification tags on different packaging, Package. Technol. Sci., 25 (**2012**) 7, 373–384
[8] U. Kavčič, M. Maček, T. Muck, Impact study of disturbance on readability of two similar UHF RFID tags, Inf. MIDEM, 41 (**2011**) 3, 197–201
[9] X. Nie, H. Wang, J. Zou, Inkjet printing of silver citrate conductive ink on PET substrate, Applied Surface Science, 261 (**2012**), 554–560
[10] A. Kanso, E. Arnaud, T. Monediere, M. Thevenot, E. Beaudrouet, C. Dossou-yovo, R. Noguera, Inkjet printing of Coplanar Wire-Patch antenna on a flexible substrate, 15th International Symposium on Antenna Technology and Applied Electromagnetics, Toulouse, 2012, 1–4
[11] J. Li, B. An, J. Qin, Y. Wu, Nano copper conductive ink for RFID application, International Symposium on Advanced Packaging Materials, Xiamen, 2011, 91–93
[12] V. Radonic, K. Palmer, G. Stojanovic, V. Crnojevic-Bengin, Flexible Sierpinski Carpet Fractal Antenna on a Hilbert Slot Patterned Ground, International Journal of Antennas and Propagation, Vol. 2012, Article ID 980916, 2012, doi: 10.1155/2012/980916
[13] L. B. Keng, W. L. Lai, C. W. A. Lu, B. Salam, Processing and characterization of flexographic printed conductive grid, Electronics Packaging Technology Conference, Singapore, 2011, 517–520
[14] D. A. Alsaid, E. Rebrosova, M. Joyce, M. Rebros, M. Z. Atashbar, B. Bazuin, Gravure Printing of ITO Transparent Electrodes for Applications in Flexible Electronics, Journal of Display Technology, 8 (**2012**), 391–396
[15] S. L. Merilampi, P. Ruuskanen, T. Björninen, L. Sydänheimo, L. Ukkonen, Characterization of UHF RFID tags fabricated directly on convex surfaces by pad printing, International Journal of Advanced Manufacturing Technology, 53 (**2011**), 577–591
[16] Z. J. Tang, Y. G. He, Y. Wang, Broadband RFID tag antenna with quasi-isotropic radiation performance, AEU-International Journal of Electronics and Communications, 65 (**2011**), 859–863
[17] D. M. Dobkin, The RF in RFID, Passive UHF RFID in Practice, Elsevier, 2008
[18] K. Finkenzeller, D. Muller, RFID Handbook: Fundamentals and Applications in Contactless Smart Cards, Radio Frequency Identification and Near-Field Communication, 3rd edition, John Wiley & Sons, Inc., 2010
[19] A. Syed, K. Demarest, D. D. Deavours, Effects of antenna material on the performance of UHF RFID tags, IEEE International Conference on RFID, Grapevine, 2007, 57–62
[20] C. A. Balanis, Antenna Theory: Analysis and Design, 3rd edition, John Wiley & Sons, Inc., 2005